

## DETERMINATION OF THE EFFECT OF $\text{TiO}_2$ ON THE DYNAMIC BEHAVIOR OF SCALED CONCRETE CHIMNEY BY OMA

### DOLOČITEV VPLIVA $\text{TiO}_2$ NA DINAMIČNO OBNAŠANJE POMANJŠANEGA MODELA CEMENTNEGA DIMNIKA S PROGRAMSKIM ORODJE OMA

Sertaç Tuhta, Furkan Günday\*

Ondokuz Mayıs University, Faculty of Engineering, Department of Civil Engineering, Atakum/Samsun, Turkey

*Prejem rokopisa – received: 2021-03-01; sprejem za objavo – accepted for publication: 2021-03-15*

doi:10.17222/mit.2021.059

In this article, the dynamic parameters (frequencies, mode shapes, damping ratios) of a scaled concrete chimney and the dynamic parameters (frequencies, mode shapes, damping ratios) of the entire outer surface of the 80-micron-thick titanium dioxide are compared using the operational modal analysis method. Ambient excitation was provided from micro tremor ambient vibration data at ground level. Enhanced Frequency Domain Decomposition (EFDD) is used for the output-only modal identification. From this study, very best correlation is found between the mode shapes. Titanium dioxide applied to the entire outer surface of the scaled concrete chimney has an average of 16.34 % difference in frequency values and 9.81 % in damping ratios, proving that nanomaterials can be used to increase the rigidity in chimneys, in other words, for reinforcement. Another important result determined in the study is that it has been observed that the adherence of titanium dioxide and similar nanomaterials mentioned in the introduction to concrete chimney surfaces is at the highest level.

Keywords: Operational Modal Analysis, nanomaterial, EFDD,  $\text{TiO}_2$

V članku avtorji opisujejo primerjavo dinamičnih parametrov (frekvence, modelane oblike, razmerja dušenja) pomanjšanega modela betonskega dimnika in dinamične parametre dimnika s prevleko celotne zunanje površine z 80 mikrometrov debelo plastjo titanovega dioksida. Primerjavo so izvedli z uporabo metode operacijske modalne analize (OMA). Okoljsko vzbujanje so dobili s pomočjo podatkov za mikro tresenje na površini tal. Uporabili so stopnjevano frekvenčno domensko dekompozicijo (EFDD) samo za izhodno modalno identifikacijo. S pomočjo predstavljene študije so našli najboljšo korelacijo med modelanimi oblikami. S titanovim dioksidom prevlečena celotna zunanja površina s modela pomanjšanega betonskega dimnika se je v povprečju razlikovala po frekvenčnih vrednostih za 16,34 % in za 9,81 % v razmerjih dušenja. Avtorji so s tem dokazali, da se nanomateriali lahko uporabijo za povečanje togosti dimnikov, z drugimi besedami, da se lahko uporabijo za njihovo ojačitev. Drug pomemben rezultat te študije je opažanje, da je zelo velika oziroma močna povezanost titanovega oksida in drugih podobnih nano materialov z betonsko osnovo površine dimnika.

Ključne besede: operacijska modalna analiza, nanomaterial, EFDD,  $\text{TiO}_2$

## 1 INTRODUCTION

Since nanotechnology is an ever-evolving field, it is difficult to make a general definition. However, according to the definition that everyone agrees with, the creation of materials and devices by controlling the substance is called nanotechnology. At the level of atoms, molecules and superamolecular (nanoscale) structures, in other words, it is possible to express it as the use of very small material particles to create new, large-scale materials. Products produced using nanotechnologies are called nanomaterials. Depending on the size, nanotechnology is defined as the study and use of structures between 1 nm and 100 nm in size. Different things happen in nano-level processing, for example, gravity becomes insignificant, electrostatic forces and quantum effects come into play. Another important point is that as a result of the use of particles on the nanoscale, the ratio of the atoms on the surface increases compared to the ones

inside, causing the material properties to change. Nanotechnology can produce products with many unique properties that can improve existing building materials: lighter and stronger structural composites, reduced-maintenance coatings, more useful cement-based materials, products with better thermal insulation properties, etc. The use of nanomaterials in the composition of some materials such as cement, etc. will be beneficial in air conditioning and energy efficiency. In addition, nanomaterials applied to the surfaces of structural elements of buildings can contribute to environmental cleaning and energy generation through photocatalytic reactions.<sup>1</sup> Thanks to nanotechnology, concrete can be stronger, more durable and easier to place, steel can be made tougher, glass self-cleaning, and paints can be made more insulating and water-repellent. Nanomaterials and nanotechnologies have attracted considerable scientific interest due to new potential uses of nanometer-scale particles and hence the large amount of funding and effort. Compared to other large industrial sectors, the construction industry has lagged behind in its potential to

\*Corresponding author's e-mail:  
furkan.gunday@omu.edu.tr (Furkan Günday)

benefit from nanotechnology. Reports on the use of nanotechnology in construction materials, the potential uses of nanotechnology in terms of construction and the development of building materials are listed as follows. Using nanoparticles, carbon nanotubes and nanofibers to increase the strength and durability of cement composites and to reduce environmental pollution. Cheap and corrosion-free steel production. Product production with ten times the performance of existing thermal insulation materials. The production of coatings that enable self-cleaning and self-color change to minimize energy consumption. Because macro properties can change at the nanoscale and it is possible to produce significantly new materials and processes. Discussions on the application of nanotechnology in civil engineering, especially in construction, are extremely important. However, most of the advances in nanotechnology are civil engineering. Furthermore, many of the advances in nanotechnology have the potential to apply in civil engineering. In the light of the information mentioned above, carbon nanotubes, one of the most used nanomaterials in the field of civil engineering, are in the form of a cylindrical carbon and it takes its name from the nanometer diameter. Nanotubes have superior strength and unique electrical properties, as well as efficient thermal properties. For example, it has five times the strength of steel and its density is one-sixth. The mechanical strength of carbon nanotubes in civil engineering, crack prevention in concrete, etc. It is very popular due to its properties. Some of the studies on nanomaterials used in this study are as follows. Longitudinal vibration of nanorods embedded in an elastic medium with elastic restraints at both ends.<sup>2</sup> Axial vibration analysis of cracked nanorods with arbitrary boundary conditions.<sup>3</sup> Torsion of nonlocal bars with equilateral triangle cross-sections.<sup>4</sup> Free vibration of FG nanobeam using a finite-element method.<sup>5</sup> Torsional vibration analysis of nanorods with elastic torsional restraints using non-local elasticity theory.<sup>6</sup> Buckling analysis of non-local timoshenko beams using Fourier series.<sup>7</sup> A compact analytical method for vibration of micro-sized beams with different boundary conditions.<sup>8</sup> In these studies, the authors examined the mechanical properties of various nanomaterials. Another nanomaterial, titanium dioxide nanoparticles, is added to concrete to improve its properties. This white pigment is used as a very good reflective coating or added to paints, cements and windows for its sterilizing properties. The multifunctionality of titanium dioxide is of great interest for both contemporary science and technology.<sup>9</sup> Titanium and its alloys are some of the most widely used implant materials because of their low toxicity, biocompatibility and mechanical properties.<sup>10</sup> Coatings of pure titanium dioxide (TiO<sub>2</sub>) are multifunctional due to their good properties, such as high hardness, density, tensile bond strength, chemical stability, resistance to oxidation and wear, good biocompatibility and antibacterial properties, and photo-electrochemical properties and a high dielec-

tric constant.<sup>11</sup> It was shown that sub-micron TiO<sub>2</sub> particles significantly enhance the glass-transition temperature,<sup>12</sup> thermal oxidative stability, tensile strength and Young's modulus of epoxy polymers.<sup>13</sup> The need for the light-weight and high-performance materials is increased day by day due to the increase in the application areas such as automotive, aerospace, deep-ocean, nuclear-energy generation, structural applications, etc., that have led to the invention of hybrid materials in the form of composites.<sup>14</sup> Titanium dioxide breaks down organic pollutants, volatile organic compounds and bacterial membranes through powerful photocatalytic reactions and reduces the proportion of air pollutants when applied to external surfaces. As it is hydrophilic, it provides self-cleaning feature to the applied surfaces. The concrete surfaces obtained have a white color that preserves their whiteness very effectively. Silicon dioxide particles, on the other hand, have the ability to increase the compressive strength significantly. By filling the pores between large fly ash and cement particles, they allow the production of concrete containing large fly-ash volumes at an early age. Nano-silica shortens the setting time of mortar compared to silica fume (microsilica) and reduces mixing water and segregation by improving the cohesion. Zinc oxides are preferred because of their semiconductor and piezoelectric properties. In building materials, they are added to a variety of products, including plastics, ceramics, glass, cement, rubber, paints, adhesives, sealants, pigments, and flame retardants. Zinc oxide used in concrete production improves the concrete's processing time and resistance to water. Another nanomaterial, alumina, reacts with calcium hydroxide produced from the hydration of calcium silicates. The rate of pozzolanic reaction is proportional to the amount of surface area available for the reaction. The addition of high-purity nano-alumina improves the properties of concretes in terms of higher tensile stress and flexural strength. Cement can advantageously be displaced in the concrete mix with nano-alumina particles up to a maximum limit of 2.0 % with an average particle sizes of 15 nm; optimum nano-alumina particle content is achieved with 1.0 % replacement. For this reason, a study that has no examples in the literature was conducted here. The dynamic parameters (frequencies, mode shapes, damping ratios) of a scaled concrete chimney were found by the operational modal analysis method. In the continuation of the research, the upper surface of this chimney was coated with titanium dioxide (80 µm), and its dynamic parameters (frequencies, mode shapes, damping ratios) were found again by the operational modal analysis method and compared. The reason for using titanium dioxide in the study is that its mechanical properties are as good as conventional materials (AFRP, BFRP, CFRP, GFRP, etc.) used in reinforcement. Thanks to the research, details that will help people who work on this subject are included. The use of other nanomaterials such as titanium dioxide as a reinforcement element in



concrete, reinforced concrete, steel, composite-type structures is being investigated, and the results of these studies will be presented later.

Ambient vibration testing (also called Operational Modal Analysis) is the most economical non-destructive testing method to acquire vibration data from large civil engineering structures for Output-Only Modal Identification.<sup>15</sup> The general characteristics of the structural response (appropriate frequency, displacement, velocity, acceleration), suggested the measuring quantity (such as velocity or acceleration) depends on the type of vibrations (Traffic, Acoustic, Machinery inside, Earthquakes, Wind...), which are given in Vibration of Buildings 1990.<sup>16</sup>

In general, operational modal analysis is used to determine the damage levels of the existing structures, to check the validity of the assumptions made while constructing the finite-element model, to update the initial numerical model of the existing structures according to the experimental data, to determine the dynamic characteristics of the structures by the experimental modal analysis method when the numerical model of the existing structures cannot be formed and to follow the structural health is widely used in the process.<sup>17–22</sup> It was observed that three types of definitions were used in the engineering structures: modal parameter identification; structural-modal parameter identification; control-model identification methods are used. In the frequency domain, the identification is based on the singular value decomposition of the spectral density matrix and it is denoted as the Frequency Domain Decomposition (FDD) and its further development Enhanced Frequency Domain Decomposition (EFDD). In the time domain there are three different implementations of the Stochastic Subspace Identification (SSI) technique: Unweighted Principal Component (UPC); Principal component (PC); Canonical Variety Analysis (CVA) is used for the modal updating of the structure.<sup>23–26</sup>

It is necessary to estimate the sensitivity of the reaction of the examined system to a change of the random or fuzzy parameters of a structure. Investigated measurement-noise perturbation influences the identified system modal and the physical parameters. The estimated measurement noise border, for which the identified system parameters are acceptable for the validation of the finite-element model of the examined system. System identification is realized by observer algorithms.<sup>27–30</sup> In special cases, the observer gain may coincide with the Kalman gain. A stochastic state-space model of the structure is simulated by the Monte-Carlo method. As a result of these theoretical and experimental studies, the importance of temperature change and humidity has emerged once again from the environmental factors affecting the modal parameters. The effects of temperature and humidity on the modal parameters have been the subject of thorough examinations in the past 15 years.<sup>31–34</sup>

For this purpose, the dynamic parameters (frequencies, mode shapes, damping ratios) of the scaled concrete structure and the dynamic parameters (frequencies, mode shapes, damping ratios) of the entire outer surface of the 80- $\mu$ m-thick titanium dioxide are compared using the operational modal analysis method. Ambient excitation was provided from the recorded micro tremor ambient vibration data at ground level. Enhanced Frequency Domain Decomposition (EFDD) is used for the output-only modal identification.

## 2 MODAL PARAMETER EXTRACTIONS (EFDD)

The FDD ambient modal identification is an extension of the Basic Frequency Domain (BFD) technique or called the Peak-Picking technique. This method uses the fact that modes can be estimated from the spectral densities calculated, in the case of a white-noise input, and a lightly damped structure. It is a non-parametric technique that determines the modal parameters directly from the signal processing. The FDD technique estimates the modes using a Singular Value Decomposition (SVD) of each of the measurement datasets. This decomposition corresponds to a Single Degree of Freedom (SDOF) identification of the measured system for each singular value.<sup>35</sup>

The Enhanced Frequency Domain Decomposition technique is an extension to the Frequency Domain Decomposition (FDD) technique. This technique is a simple technique that is extremely basic to use. In this technique, modes are easily picked locating the peaks in Singular Value Decomposition (SVD) plots calculated from the spectral density spectra of the responses. The FDD technique is based on using a single frequency line from the Fast Fourier Transform analysis (FFT), the accuracy of the estimated natural frequency based on the FFT resolution and no modal damping is calculated. On the other hand, the EFDD technique gives an advanced estimation of both the natural frequencies, the mode shapes and includes the damping ratios.<sup>36</sup> In the EFDD technique, the single degree of freedom (SDOF) Power Spectral Density (PSD) function, identified about a peak of resonance, is taken back to the time domain using the Inverse Discrete Fourier Transform (IDFT). The natural frequency is acquired by defining the number of zero crossings as a function of time, and the damping by the logarithmic decrement of the correspondent single degree of freedom (SDOF) normalized auto correlation function.<sup>37</sup>

In this study the modal parameter identification was implemented by the Enhanced Frequency Domain Decomposition. The EFDD method formulation used in most of the studies referencing this study in the introduction is as follows. The relationship between the input and responses in the EFDD technique can be written as, in this method, the unknown input is represented with  $x(t)$  and measured output is represented with  $y(t)$

$$[G_{yy}(j\omega)] = [H(j\omega)]^* [G_{xx}(j\omega)] [H(j\omega)]^T \quad (1)$$

where  $G_{xx}(j\omega)$  is the  $r \times r$  Power Spectral Density (PSD) matrix of the input.  $G_{yy}(j\omega)$  is the  $m \times m$  Power Spectral Density (PSD) matrix of the output,  $H(j\omega)$  is the  $m \times r$  Frequency Response Function (FRF) matrix, and  $*$  and superscript  $T$  denotes the complex conjugate and transpose, respectively. The FRF can be reduced to a pole/residue form as follows:

$$[H(\omega)] = \frac{[Y(\omega)]}{[X(\omega)]} = \sum_{k=1}^m \frac{[R_k]}{j\omega - \lambda_k} + \frac{[R_k]^*}{j\omega - \lambda_k^*} \quad (2)$$

where  $n$  is the number of modes  $\lambda_k$  is the pole and,  $R_k$  is the residue. Then Equation (1) becomes as:

$$G_{yy}(j\omega) = \sum_{k=1}^n \sum_{s=1}^n \left[ \frac{[R_k]}{j\omega - \lambda_k} + \frac{[R_k]^*}{j\omega - \lambda_k^*} \right] \bar{H}$$

$$G_{xx}(j\omega) = \left[ \frac{[R_s]}{j\omega - \lambda_s} + \frac{[R_s]^*}{j\omega - \lambda_s^*} \right] \bar{H} \quad (3)$$

where  $s$  the singular values, superscript  $H$  denotes the complex conjugate and transpose. Multiplying the two partial fraction factors and making use of the Heaviside partial fraction theorem, after some mathematical manipulations, the output PSD can be reduced to a pole/residue form as follows:

$$[G_{yy}(j\omega)] =$$

$$= \sum_{k=1}^n \frac{[A_k]}{j\omega - \lambda_k} + \frac{[A_k]^*}{j\omega - \lambda_k^*} + \frac{[B_k]}{-j\omega - \lambda_k} + \frac{[B_k]^*}{-j\omega - \lambda_k^*} \quad (4)$$

where  $A_k$  is the  $k$  th residue matrix of the output PSD. In the EFDD identification, the first step is to estimate the PSD matrix. The estimation of the output PSD known at discrete frequencies is then decomposed by taking the SVD (singular value decomposition) of the matrix;

$$G_{yy}(j\omega_i) = U_i S_i U_i^H \quad (5)$$

where the matrix  $U_i = [u_{i1}, u_{i2}, \dots, u_{im}]$  is a unitary matrix holding the singular vectors  $u_{ij}$  and  $s_{ij}$  is a diagonal matrix holding the scalar singular values. The first singular vector  $u_{ij}$  is an estimation of the mode shape. The PSD function is identified around the peak by comparing the mode shape estimation  $u_{ij}$  with the singular vectors for the frequency lines around the peak. From the piece of the SDOF density function obtained around the peak of the PSD, the natural frequency and the damping can be obtained.

### 3 DESCRIPTION OF SCALED CONCRETE CHIMNEY

The scaled concrete chimney was produced in the Ondokuz Mayıs University Civil Engineering Laboratory. The mechanical properties of the concrete used are as follows: modulus of elasticity  $E = 28$  GPa, Poisson ra-

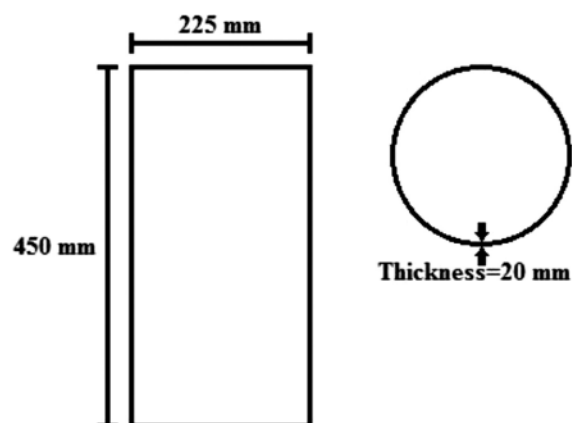


Figure 1: Illustration of scaled concrete chimney

tio  $\mu = 0.2$ , mass per unit volume  $\rho = 2447.3$  kg/m<sup>3</sup>. The dimensions of the building are shown in Figure 1.

### 4 OPERATIONAL MODAL ANALYSIS OF SCALED CONCRETE CHIMNEY

Three accelerometers are used to measure the ambient vibrations. One of them is always assigned as the reference sensor located at the bottom of the shear wall. The acceleration record was measured in two datasets. For the two datasets, 1 and 2 accelerometers were used, respectively. Accelerometers were calibrated and used, thus preventing possible measurement errors. A total of 100 minutes were recorded for each dataset. Selected measurement points and directions are shown in Figure 2. Ambient stimulation was achieved using micro-tremor data recorded at ground level.

The data-acquisition computer provides the ambient vibration records. During measurements, the data files from the previous setup are transferred to the computer for data analysis by using a software package. However, in the case there is a display of unexpected signal drifts or unwanted noise or corrupted for some unknown rea-

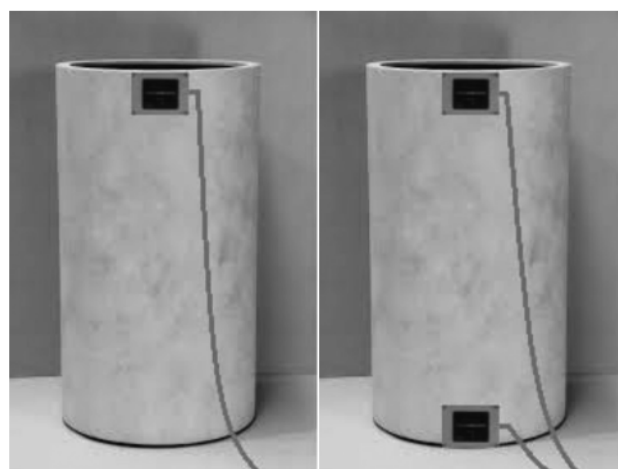
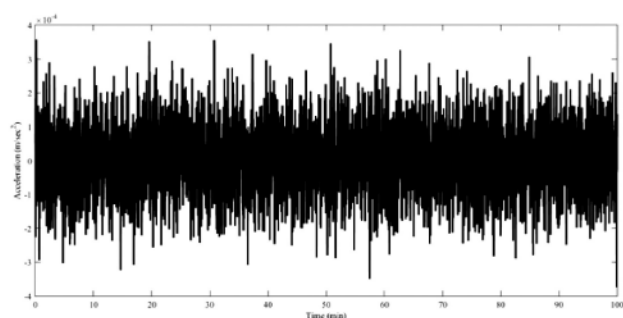


Figure 2: For setup 1 and setup 2 selected measurement points and directions



**Figure 3:** Ambient excitation data from the recorded micro tremor data at ground level

sons, the data set must be discarded and measurements be repeated.

Before measurements, the cable used to connect the sensors to the data-acquisition equipment must be laid out. Following each measurement, the roving sensors are systematically located from floor to floor until the test is completed (**Figure 2**). The equipment used for the measurement includes three sensebox accelerometers (with both x and y directional measurements) and güralp systems seismometer and MATLAB data-acquisition toolbox. For the modal parameter estimation from the ambient vibration data, the operational modal analysis OMA software ARTEMIS Extractor is used.

The eigen frequencies are found as the peaks of non-parametric spectrum estimates when the simple peak-picking method (PPM) is used. This frequency-selection procedure becomes a subjective task in the case of noisy test data, weakly excited modes and relatively close eigen frequencies. Also, for the damping-ratio estimation, the related half-power bandwidth method is not favorable. This why the most popular and useful algorithm to use is the frequency-domain one, because of its convenience and operating speed.

Ambient excitation data from the recorded micro tremor data at ground level is given in **Figure 3**.

Singular values of the spectral density matrices for scaled concrete chimney are given in **Figure 4**.

The first five modes of the mode shapes of the scaled concrete chimney are given in **Figures 5 to 9**.

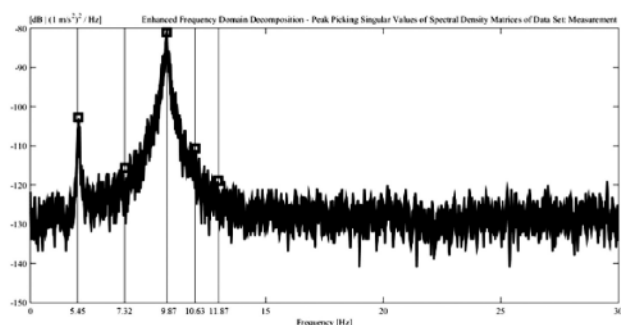


**Figure 4:** Singular values of spectral density matrices for scaled concrete chimney



**Figure 5:** 1<sup>st</sup> mode shape ( $f = 5.45$  Hz,  $\xi = 1.04$ )



**Figure 6:** 2<sup>nd</sup> mode shape ( $f = 7.32$  Hz,  $\xi = 0.88$ )



**Figure 7:** 3<sup>rd</sup> mode shape ( $f = 9.87$  Hz,  $\xi = 0.71$ )



**Figure 8:** 4<sup>th</sup> mode shape ( $f = 10.63$  Hz,  $\xi = 0.82$ )



**Figure 9:** 5<sup>th</sup> mode shape ( $f = 11.87$  Hz,  $\xi = 0.64$ )



The natural frequencies acquired from all the measurement setups are given in **Table 1**.

**Table 1:** Operational modal analysis result at the scaled concrete chimney

Mode number	1	2	3	4	5
Frequency (Hz)	5.45	7.32	9.87	10.63	11.87
Modal damping ratio ( $\xi$ )	1.04	0.88	0.71	0.82	0.64

When all the measurements are examined, it can be seen that the best accordance is found between the experimental mode shapes. In addition, when both setup sets are experimentally identified the modal parameters are checked with each other, it can be seen that there is a best agreement between the mode shapes in the experimental modal analyses.

## 5 OPERATIONAL MODAL ANALYSIS OF COATED SCALED CONCRETE CHIMNEY

In the case of the coated scaled concrete chimney, the following studies are made on it to check and examine the efficiency of using the TiO<sub>2</sub> coating: entire outer surface of the 80-micron thick of the chimney are coated with multi-layer TiO<sub>2</sub> coating. TiO<sub>2</sub> coating and its components YKS is product of YKS Corporation (**Figure 6**). The properties of the TiO<sub>2</sub> coating are:  $E = 23$  GPa, Poisson ratio  $\mu = 0.27$ , mass per unit volume  $\rho = 4078.86$  kg/m<sup>3</sup>, thickness = 80  $\mu$ m.

The entire outer surface of the scaled concrete chimney is covered with many layers of titanium dioxide. The surface is expected to dry during each application. Approximately 1 hour of curing is required in order to prepare a surface for application of titanium dioxide. After these setups, ambient vibration tests are followed by curing to obtain the experimental dynamic characteristics, similar to previously used properties in order to obtain comparative measurements. SVSDM are shown in **Figure 10**.

The first five modes of mode shapes of coated scaled concrete chimney are given in **Figure 11, 12, 13, 14, 15**.

It is clear that using titanium dioxide seems to be very effective for strengthening concrete members along

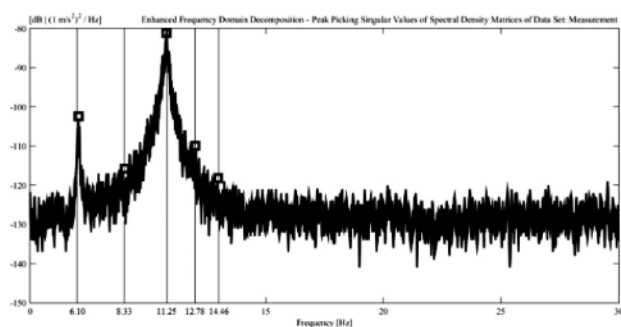


**Figure 10:** Singular values of spectral density matrices for coated scaled concrete chimney



**Figure 11:** 1<sup>st</sup> mode shape ( $f = 6.10$  Hz,  $\xi = 0.97$ )



**Figure 12:** 2<sup>nd</sup> mode shape ( $f = 8.33$  Hz,  $\xi = 0.85$ )



**Figure 13:** 3<sup>rd</sup> mode shape ( $f = 11.25$  Hz,  $\xi = 0.62$ )



**Figure 14:** 4<sup>th</sup> mode shape ( $f = 12.78$  Hz,  $\xi = 0.73$ )



**Figure 15:** 5<sup>th</sup> mode shape ( $f = 14.46$  Hz,  $\xi = 0.54$ )

with increasing stiffness; this research aims to determine how TiO<sub>2</sub> implementation affects the structural response of a scaled concrete chimney by changing the dynamic characteristics. **Table 2** shows the identified natural frequencies and modal damping ratios.

**Table 2:** Operational modal analysis result at the coated scaled concrete chimney

Mode number	1	2	3	4	5
Frequency (Hz)	6.10	8.33	11.25	12.78	14.46
Modal damping ratio ( $\xi$ )	0.97	0.85	0.62	0.73	0.54

**Table 3** shows comparison of existing and coated chimney frequency results. E is the existing chimney and C is the coated chimney in **Table 3**.

**Table 3:** Comparison of existing and coated chimney frequency results

Mode number	1	2	3	4	5
Frequency (Hz)-E	5.45	7.32	9.87	10.63	11.87
Frequency (Hz)-C	6.10	8.33	11.25	12.78	14.46
Difference (%)	11.92	13.79	13.98	20.22	21.81

**Table 4** shows comparison of existing and coated chimney damping ratio results.

**Table 4:** Comparison of existing and coated chimney damping ratio results

Mode number	1	2	3	4	5
Modal damping ratio ( $\xi$ )-E	1.04	0.88	0.71	0.82	0.64
Modal damping ratio ( $\xi$ )-C	0.97	0.85	0.62	0.73	0.54
0Difference (%)	6.73	3.40	12.67	10.97	15.62

## 6 CONCLUSIONS

In this research, we conducted both operational modal analysis of an existing scaled concrete chimney and a titanium dioxide coated scaled concrete chimney. Comparing the result of study, the followings are noticed:

- From the ambient vibration test, the first five natural frequencies are attained experimentally, which range between 5 Hz and 15 Hz.
- When comparing the existing and coated scaled concrete chimney results, it is clear that there is very best agreement between mode shapes.
- It has been determined that there is an average of 16.34 % difference between the frequency values of the existing scaled concrete chimney and the titanium-dioxide-coated scale concrete chimney.
- It has been determined that there is an average of 9.81 % difference between the damping ratios of the existing scale concrete chimney and the titanium dioxide coated scale concrete chimney.
- Titanium dioxide applied to the entire outer surface (80  $\mu$ m) of the scaled concrete chimney has an average of 16.34 % difference in frequency values (**Table**

**3**) and 9.81 % in damping ratios (**Table 4**), proving that nanomaterials can be used to increase rigidity in chimneys, in other words, for reinforcement.

- Another important result determined in the study is that it has been observed that the adherence of titanium dioxide and similar nanomaterials mentioned in the introduction to concrete chimney surfaces is at the highest level.

## 7 REFERENCES

- <sup>1</sup> Ş. D. Akbaş, Modal analysis of viscoelastic nanorods under an axially harmonic load, *Advances in Nano Research*, 8 (2020) 4, 277–282, doi:10.12989/anr.2020.8.4.277
- <sup>2</sup> M. Ö. Yayli, F. Yanik, S. Y. Kandemir, Longitudinal vibration of nanorods embedded in an elastic medium with elastic restraints at both ends, *Micro & Nano Letters*, 10 (2015) 11, 641–644, doi:10.1049/mnl.2014.0680
- <sup>3</sup> M. Ö. Yayli, A. E. Cercevik, Axial vibration analysis of cracked nanorods with arbitrary boundary conditions, *Journal of Vibro-engineering*, 17 (2015) 6, 2907–2921
- <sup>4</sup> M. Ö. Yayli, Torsion of nonlocal bars with equilateral triangle cross sections, *Journal of Computational and Theoretical Nanoscience*, 10 (2013) 2, 376–379, doi:10.1166/jctn.2013.2707
- <sup>5</sup> B. Uzun, M. Ö. Yayli, B. Deliktaş, Free vibration of FG nanobeam using a finite-element method, *Micro & Nano Letters*, 15 (2020) 1, 35–40, doi:10.1049/mnl.2019.0273
- <sup>6</sup> M. Ö. Yayli, Torsional vibration analysis of nanorods with elastic torsional restraints using non-local elasticity theory, *Micro & Nano Letters*, 13 (2018) 5, 595–599, doi:10.1049/mnl.2017.0751
- <sup>7</sup> H. Kadioglu, M. Ö. Yayli, Buckling analysis of non-local Timoshenko beams by using Fourier series, *International Journal of Engineering and Applied Sciences*, 9 (2017) 4, 89–99, doi:10.24107/ijeas.362242
- <sup>8</sup> M. Ö. Yayli, A compact analytical method for vibration of micro-sized beams with different boundary conditions, *Mechanics of Advanced Materials and Structures*, 24 (2016) 6, 496–508, doi:10.1080/15376494.2016.1143989
- <sup>9</sup> S. Cherneva, R. Iankov, N. Radic, B. Grbic, M. Datcheva, D. Stoychev, Nano-indentation investigations of the mechanical properties of thin TiO<sub>2</sub>, WO<sub>3</sub> and their composites layers, deposited by spray pyrolysis, *Mater. Tehnol.*, 51 (2017) 1, 75–83, doi:10.17222/mit.2015.216
- <sup>10</sup> M. Kulkarni, J. Šepitka, I. Junkar, M. Benčina, N. Rawat, A. Mazare, C. Rode, S. Gokhale, P. Schmuki, M. Daniel, A. Iglic, Mechanical properties of anodic titanium dioxide nanostructures, *Mater. Tehnol.*, 55 (2021) 1, 19–24, doi:10.17222/mit.2020.109
- <sup>11</sup> M. Mrdak, D. Bajic, D. Veljic, M. Rakin, Mechanical and structural characteristics of atmospheric plasma-sprayed multifunctional TiO<sub>2</sub> coatings, *Mater. Tehnol.*, 54 (2020) 6, 807–812, doi:10.17222/mit.2020.052
- <sup>12</sup> Z. Rubab, A. Afzal, H. M. Siddiqi, S. Saeed, Preparation, Characterization, and Enhanced Thermal and Mechanical Properties of Epoxy-Titania Composites, *Scientific World Journal*, 2014 (2014) 5, 1–7, doi:10.1155/2014/515739
- <sup>13</sup> A. Kocijan, M. Conradi, Č. Donik, Corrosion resistance of superhydrophilic and superhydrophobic TiO<sub>2</sub>/epoxy coatings on AISI 316L stainless steel, *Mater. Tehnol.*, 52 (2018) 4, 383–388, doi:10.17222/mit.2017.191
- <sup>14</sup> G. Elango, B. Raghunath, K. Palanikumar, Experimental analysis of the wear behavior of hybrid metal-matrix composites of LM25Al with equal volumes of SiC + TiO<sub>2</sub>, *Mater. Tehnol.*, 48 (2014) 6, 803–810
- <sup>15</sup> F. Günday, GFRP Retrofitting Effect on the Dynamic Characteristics of Model Steel Structure Using SSI, *International Journal of Ad-*

- vance Engineering and Research Development, 5 (2018) 4, 1160–1173
- <sup>16</sup> F. Günday, OMA of RC Industrial Building Retrofitted with CFRP using SSI, International Journal of Advance Engineering and Research Development, 5 (2018) 5, 759–771
- <sup>17</sup> K. F. Alvin, K. C. Park, Second-order structural identification procedure via state-space-based system identification, AIAA Journal, 32 (1994) 2, 397–406, doi:10.2514/3.11997
- <sup>18</sup> D. H. Tseng, R. W. Longman, J. N. Juang, Identification of the structure of the damping matrix in second order mechanical systems, Spaceflight Mechanics, 87 (1994) 1, 167–190
- <sup>19</sup> F. A. Aliev, V. B. Larin, Optimization of Linear Control Systems: Analytical Methods and Computational Algorithms; CRC Press, New York, USA, 1998
- <sup>20</sup> L. Ljung, System Identification: Theory for the User; Prentice Hall, New York, USA, 1999
- <sup>21</sup> H. Lus, M. De Angelis, R. Betti, R. W. Longman, Constructing second-order models of mechanical systems from identified state space realizations, Part I: Theoretical discussions, Journal of Engineering Mechanics, 129 (2003) 5, 477–488, doi:10.1061/(ASCE)0733-9399(2003)129:5(477)
- <sup>22</sup> G. D. Roeck, The state-of-the-art of damage detection by vibration monitoring: the SIMCES experience, Journal of Structural Control, 10 (2003) 2, 127–134, doi:10.1002/stc.20
- <sup>23</sup> A. Sestieri, S. R. Ibrahim, Analysis of errors and approximations in the use of modal coordinates, Journal of Sound and Vibration, 177 (1994) 2, 145–157, doi:10.1006/jsvi.1994.1424
- <sup>24</sup> E. Balmes, New results on the identification of normal modes from experimental complex modes, Mechanical Systems and Signal Processing, 11 (1997) 2, 229–243, doi:10.1006/mssp.1996.0058
- <sup>25</sup> J. S. Bendat, Nonlinear Systems Techniques and Applications; Wiley, New York, USA, 1998
- <sup>26</sup> T. Marwala, Finite Element Model Updating Using Computational Intelligence Techniques: Applications to Structural Dynamics; Springer, Berlin, 2010
- <sup>27</sup> R. E. Kalman, A new approach to linear filtering and prediction problems, Journal of Basic Engineering, 82 (1960) 1, 35–45, doi:10.1115/1.3662552
- <sup>28</sup> M. D. Trifunac, Comparisons between ambient and forced vibration experiments, Earthquake Engineering and Structural Dynamics, 1 (1972) 2, 133–150, doi:10.1002/eqe.4290010203
- <sup>29</sup> S. R. Ibrahim, Random decrement technique for modal identification of structures, Journal of Spacecraft and Rockets, 14 (1977) 11, 696–700, doi:10.2514/3.57251
- <sup>30</sup> J. N. Juang, Applied System Identification; Prentice Hall, New York, USA, 1994
- <sup>31</sup> A. A. Kasimzade, S. Tuhta, Application of OMA on the bench-scale earthquake simulator using micro tremor data, Structural Engineering and Mechanics, 61 (2017) 2, 267–274, doi:10.12989/sem.2017.61.2.267
- <sup>32</sup> A. A. Kasimzade, S. Tuhta, OMA of model steel structure retrofitted with CFRP using earthquake simulator, Earthquakes and Structures, 12 (2017) 6, 689–697, doi:10.12989/eas.2017.12.6.689
- <sup>33</sup> S. Tuhta, GFRP retrofitting effect on the dynamic characteristics of model steel structure, Steel and Composite Structures, 28 (2018) 2, 223–231, doi:10.12989/scs.2018.28.2.223
- <sup>34</sup> S. Tuhta, OMA of model chimney using Bench-Scale earthquake simulator, Earthquakes and Structures, 16 (2019) 3, 321–327, doi:10.12989/eas.2019.16.3.321
- <sup>35</sup> R. Brincker, L. Zhang, P. Andersen, Modal identification from ambient responses using frequency domain decomposition, Proceedings of the 18<sup>th</sup> International Modal Analysis Conference (IMAC), February, 2000, San Antonio, Texas, USA
- <sup>36</sup> N. J. Jacobsen, P. Andersen, R. Brincker, Using enhanced frequency domain decomposition as a robust technique to harmonic excitation in operational modal analysis, International Conference on Noise and Vibration Engineering (ISMA), September, 2006, Leuven, Belgium
- <sup>37</sup> B. Peeters, System identification and damage detection in civil engineering, Ph.D. Dissertation, Katholieke Universiteit Leuven, Leuven, Belgium, 2000